

Grounding Text-To-Image Diffusion Models For Controlled High-Quality Image Generation

Ahmad Süleyman

Department of Computer Engineering
Turkish-German University

Göksel Biricik

Department of Computer Engineering
Yıldız Technical University

Abstract

Large-scale text-to-image (T2I) diffusion models have demonstrated an outstanding performance in synthesizing diverse high-quality visuals from natural language text captions. Multiple layout-to-image models have been developed to control the generation process by utilizing a broad array of layouts such as segmentation maps, edges, and human keypoints. In this work, we present ObjectDiffusion, a model that takes inspirations from the top cutting-edge image generative frameworks to seamlessly condition T2I models with new bounding boxes capabilities. Specifically, we make substantial modifications to the network architecture introduced in ContorlNet to integrate it with the condition processing and injection techniques proposed in GLI-GEN. ObjectDiffusion is initialized with pretraining parameters to leverage the generation knowledge obtained from training on large-scale datasets. We fine-tune ObjectDiffusion on the COCO2017 training dataset and evaluate it on the COCO2017 validation dataset. Our model achieves an AP₅₀ of 46.6, an AR of 44.5, and a FID of 19.8 outperforming the current SOTA model trained on open-source datasets in all of the three metrics. ObjectDiffusion demonstrates a distinctive capability in synthesizing diverse, high-quality, high-fidelity images that seamlessly conform to the semantic and spatial control layout. Evaluated in qualitative and quantitative tests, ObjectDiffusion exhibits remarkable grounding abilities on closed-set and open-set settings across a wide variety of contexts. The qualitative assessment verifies the ability of ObjectDiffusion to generate multiple objects of different sizes and locations.

1. Introduction

Image generation is one of the most advanced research sub-fields of the relentlessly evolving Generative Artificial Intelligence (GenAI) and Deep Learning (DL). Thanks to its transformative practical applications, Generative Adversarial Networks (GANs) [14] have succeeded in draw-

ing considerable attention both in academia and industry. Diffusion-based powerful image generation models [1, 38, 50, 53] are capable of synthesizing stunningly detailed realistic images of high-quality that capture diverse visual concepts.

One major challenge that hinders the widespread adoption of generative AI in general and image generation models in particular is the difficulty of customization. Customization is an active research topic that aims to steer the image generation process towards producing controllable content that adheres to user-specified requirements. While text prompts [32, 41] are the most common type of input, it is deemed inadequate in cases that necessitate a high degree of content and style control in the synthesized image. Particularly, the image caption falls short in providing a precise description of the sizes, colors, shapes, textures, spatial alignments, and interactions between the objects present in the synthesized image. This limitation prompted computer vision researchers to adopt and integrate more effective types of control formats, in conjunction with the naive caption to achieve a greater degree of controllability over the output scenes. Segmentation maps [76], normal maps [64], depth maps [48], edge maps [4, 70], human keypoints [5], bounding boxes [49], user scribbles, cartoon drawings, image styles or a combination of them are among the well-established conditioning modalities that can be leveraged to tailor the image generation.

In this work, we present ObjectDiffusion, a conditional image generative framework that augments text-to-image models (T2I) [36, 47] by incorporating new control capabilities. ObjectDiffusion can condition T2I models on object detection [49] annotations. That is, in addition to the text prompts, we condition T2I models on object labels and their corresponding bounding boxes. The object labels are not limited to a predefined set of categories, rather they can be in open-ended text format, for example, “a stripped pink full face motorcycle helmet”. ObjectDiffusion consists of two pretrained networks. The first is a locked text-to-image Stable Diffusion (SD) [50] model pretrained on

filtered high-resolution images from the LAION-5B [54] dataset. The second module is GroundNet, a parallel trainable network consisting of pretrained encoding blocks and a middle block of GLIGEN [28]. GroundNet is pretrained on Object365 [56], GoldG (Flickr and VG) [26], SBU [39], and CC3M [57] datasets but not fine-tuned on the COCO [30] dataset. GroundNet is integrated into the locked Stable Diffusion [50] base model via zero convolutional layers.

Our approach integrates the conditional architecture outline of ControlNet [73] with the grounding method established in GLIGEN by seamlessly leveraging their design concepts and techniques to advance the grounding capabilities while increasing the image quality. Specifically, the architecture of our proposed framework is inspired from ControlNet to optimally leverage the pretraining knowledge. However, since ControlNet does not support our conditional layout, the architecture and initialization of GroundNet are adopted from GLIGEN to enable processing and integrating the information of the object names and bounding boxes. We fine-tune ObjectDiffusion on the COCO2017 [30] training dataset and conduct a quantitative and qualitative evaluation on the COCO2017 [30] validation dataset.

The contributions of our work can be summarized as follows:

- We propose a cutting-edge framework and demonstrate its abilities in grounding pretrained text-to-image models on open-ended object descriptions and bounding box annotations.
- Our model ObjectDiffusion outperforms existing state-of-the-art models trained on open-source datasets on the FID [17] score, AP₅₀ score, and AR [44] score. Our framework is capable of generating controlled images with superior quality.
- We reduce the training cost substantially by effectively leveraging the generation and grounding capabilities of two pretrained models, SD and GLIGEN.
- We evaluate the performance of our model and analyze the results of the quantitative and qualitative evaluations.

2. Related Work

2.1. Diffusion Models

In 2015, Sohl-Dickstein et al. [58] established the theoretical foundation of the probabilistic diffusion model, a framework that works by iteratively adding random noise to the ground-truth images until all the structure is lost, and then learns how to denoise the perturbed images to restore their original structures through recursive runs of noise prediction neural network $\epsilon_\theta(x_t, t)$ over T time-steps. Alternative to noise prediction, score-based [59] generative models $s_\theta(x)$ sample new instances by estimating the gradients of the log probability distribution of the data $\nabla_x \log p_{\text{data}}(x)$. Diffusion models and score-based generative models can be

formalized under a unified framework [60].

Dhariwal et al. [8] demonstrated that probabilistic diffusion models [58] have outperformed the prominent GANs [14] both in quality and diversity metrics. Rombach et al. [50] presented Stable Diffusion (SD), a remarkable work that denoises the image in latent space in order to reduce the computational and memory requirements of operating in pixel-level space.

2.2. Control Layout Overview

Conditional models [28, 35, 45, 68, 72, 73, 75] empower image generative models, for the most part text-to-image models, to produce controllable outputs by extending them to accept single or multiple external layout maps, generally called conditions. Scribbles and sketches are simple and vague types of conditions that can be created conveniently by users. Segmentation maps [76], on the other hand, offer a granular control over the image content by dictating a pixel-level condition map of the image lattice. Hough lines [15] and Canny edges [4] can condition generative models to capture subtle texture and fine-grained details that can not be specified via bounding boxes and segmentation maps. Keypoints [5] is a format that allows creating images from skeletal structures that likely depict human postures. Advanced types of control formats include normal maps [64] and depth maps [48] both of which challenge the generative models by widening the conditioning task scope to integrate information about the perceived depth of images.

2.3. Conditional Image Generative Models

T2I models utilizes image caption to guide the generation process. Although simple and powerful, text prompt alone is insufficient for tailoring the generation process into creating customized outputs. To address this limitation, various layout-to-image systems [21, 29, 61, 63, 71, 74] have been proposed to use more advanced conditional modalities to enable a fine-grained control. Conditional models render complex images with style and content complying with the control layout. PITI [67] is a layout-to-image diffusion model that is trained from scratch on conditional tokens. Training generative models from scratch is inefficient and entails a very high training cost. T2I-Adopters [35] are light-weight neural network blocks borrowed from NLP [19] for facilitating fine-tuning huge T2I models on various types of guiding inputs like depth, segmentation, keypoints, sketch, and color maps. Some diffusion-based methods like ReCo [72] fine-tune a pretrained text-to-image model on bounding box and open-ended text information, however this continuous learning may cause a catastrophic loss of generation knowledge [20, 52].

To circumvent this, GLIGEN [28] proposed to freeze the weights of a pretrained SD model [50] and insert trainable gated self-attention layers [65] in the attention blocks

of the frozen SD to handle the grounding tokens. InstanceDiffusion [68] takes the grounding task one step further by proposing a framework for precise object-level control while simultaneously enhancing the image fidelity and the multi-object sampling capability. Zhang et al. [73] goes further by introducing ControlNet [73], a groundbreaking general-purpose conditional model. It achieves this by freezing the pretrained model weights and training a copy of the pretrained locked backbone model. The locked model is preceded by a sequence of convolutional layers for mapping the conditions into the trainable network. UniControl [45] can simultaneously condition on an array of conditions by embedding all task instructions using a task-aware HyperNet [16, 66]. UniControl demonstrates zero-shot conditioning capabilities of unseen control types. Uni-ControlNet builds on ControlNet to introduce unified frameworks to simultaneously handle multiple control formats. Uni-ControlNet [75] enables training and inferring with a composite of modalities without the need for separate training for each modality.

2.4. Training-Free Conditional Methods

Traditional conditional models require computationally expensive training on a dataset of image-control pairs. Training-free [11, 12, 27, 29, 61, 71, 74] methods circumvent this by performing the conditioning on pretrained T2I models during the sampling process eliminating the requirement for training or fine-tuning. BoxDiff [69] achieves the positional alignment effect by manipulating specific regions of the cross-attention map that correspond to the constraining boundary box regions. Guidance-based methods can achieve control by designing task-specific guidance procedures. For example, Layout Control Guidance [6] applies forward and backward guidance losses on the attention map to steer the sampling towards generating object-level control. Universal Guidance [3] offers a solution to avoid training a network on noisy data by leveraging available pretrained models like semantic segmentation and object recognition neural networks. The goal is to carefully design and minimize the loss function $\ell(c, f(\hat{z}_0))$ between the guidance function $f(\cdot)$ of the latent image z and the control module c .

Despite their success, training-free control approaches prolong sampling time and decrease perceptual quality, and as a result, they are usually used in combination with regular training-based conditional models.

3. Method

For controllable image generation, we introduce ObjectDiffusion, a framework that takes inspirations from two remarkable conditional models GLIGEN [28] and ControlNet [73] to seamlessly augment open-source text-to-image generation diffusion models on control layout. Concretely,

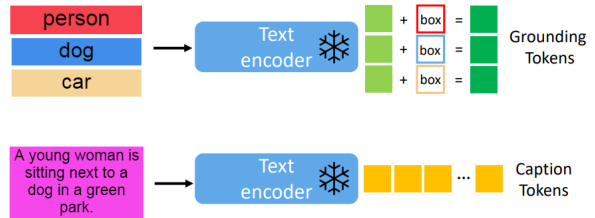


Figure 1. The grounding tokens consist of the concatenation of the CLIP [46] encoded object entities and their Fourier [34] embedded bounding boxes. Entity names do not need to be present in the caption, for example, the “car” is not mentioned in the caption. The figure is adopted and modified from [28].

we combine the powerful network architecture of ControlNet with the condition processing and injection techniques proposed in GLIGEN. Our conditional layout is the object detection annotations consisting of rectangular boxes that specify the locations of objects on the image and the associated open-ended object text that describe the content inside each of the bounding boxes [72]. ObjectDiffusion incorporates the grounding information described above with a single image caption to generate high-fidelity images where objects specified by detection labels are rendered in the regions outlined by the bounding boxes. In this section, we explain the control layout and break down the encoding techniques used to process and integrate the condition inputs into the baseline model. We represent the overall model architecture and articulate the learning objective.

3.1. Entity Grounding Layout

Due to its simplicity and effectiveness in controlling the generation process, we focus on conditioning diffusion-based models on object detection annotations. The object detection serves as a condition to ground text-to-image frameworks into rendering specific objects in specified regions of the synthesized images. In particular, our control layout consists of a set of grounding tokens, each of which is composed of one-to-one pairs of semantic and spatial information. The semantic instruction is a textual description of the object, for example, “A shiny luxury red sports car”. Each object in the image can be defined in an open-ended text format [72], rather than being limited to a predefined set of labels like COCO categories [30]. For spatial instruction, each entity is attributed by a single 2D rectangular box which determines the location of the object in the image. The box is represented in the form of an object detection rectangular box, that is, a list of two points needed to construct the detection box $[x_1, y_1, x_2, 1]$ where (x_1, y_1) is the upper-left point and (x_2, y_2) is the lower-right point. While the objects of the image are defined by the control layout, the overall image outline is specified by a single global im-

age caption, similar to T2I models.

3.2. Fusing Conditional Entities Overview

Processing Grounding Semantic Tokens: Conditional semantic tokens are strings of varying length consisting of single or multiple words. These object-level text captions are processed similar to the regular image caption. Specifically, they are encoded using a pretrained CLIP ViT-L/14 [46] text encoder. The CLIP encoder denoted as $\mathcal{E}_{\text{text}}(e)$ embeds the entity e into a tensor feature of length 768.

Processing Grounding Spatial Tokens: We embed the spatial information into an expressive periodic tensor via a Fourier embedding [34] block. The mathematical representation of Fourier transformation $F(\cdot)$ of a box $b = [x_1, y_1, x_2, y_2]$ is expressed as the following:

$$F_i(b) = [\sin(f_i \cdot x_1), \cos(f_i \cdot x_1), \dots, \dots, \sin(f_i \cdot y_2), \cos(f_i \cdot y_2)] \quad (1)$$

$$F(b) = [F_0(b), F_1(b), \dots, F_{M-1}(b)], \quad (2)$$

where $i \in \{0, 1, 2, \dots, M-1\}$

where M is the number of frequencies, and $F_i(b)$ is Fourier transformation at the f_i frequency. The output of embedding $F(b)$ is 4 (box coordinates) * 8 (frequency) * 2 (sin & cos) = 64-dimensional tensor per bounding box. The Fourier embedder does not define any trainable parameters.

Concatenating Conditional Features: For each of the grounding entity, we first concatenate the encoded text entity $\mathcal{E}_{\text{text}}(e)$ with the embedded positional information $F(b)$ into a single tensor of size 832. Then we feed this tensor as an input to a Multilayer Perceptron (MLP) [43] consisting of three fully connected linear layers of sizes (832, 515, 768) and a Sigmoid-weighted Linear Unit (SiLU) [10] :

$$o_i = \text{MLP}(\mathcal{E}_{\text{text}}(e), F(b)) \quad (3)$$

$$o = [o_1, o_2, \dots, o_N], \quad \text{where } i \in \{1, 2, \dots, N\} \quad (4)$$

The MLP transforms the concatenated grounding feature vectors from 832 to a transformer vector o_i of standard size 768. Assuming that the maximum number of entities allowed per image is a hyperparameter N , the final control vector o has the size $(N, 768)$. Figure 1 illustrates the processing of grounding information and caption.

Integrating Conditional Features: To inject the extracted control features o into the standard transformer blocks of LDM [50], we follow GLIGEN and insert a new gated self-attention SA (\cdot) layer between the self-attention and the cross-attention of the transformer block [2]. The gated self-attention layer takes both the intermediate latent visual features v and the external control features o as inputs and integrates them as shown in the equation:

$$v = v + \tanh(\gamma) \cdot \text{SA}([v, o]) \quad (5)$$

3.3. Model Architecture

Our model architecture is illustrated in Figure 2. We start with a pretrained Stable Diffusion (SD) [50] model that enables conditioning image generative diffusion models on image captions but does not support object detection data defined in the Section 3.1 as a grounding input. We lock the whole SD model and clone the encoder blocks and middle block, but not the decoder blocks, from the pretrained model into a trainable network [73]. This allows us to leverage the generation knowledge learned from training on a massive dataset. To equip our model with conditional capabilities, we introduce some modifications to the copied network structure. In particular, we insert gated self-attention (GSA) layers, implemented by $\tanh(\gamma)$ [9], into each of the attention blocks of the trainable network [28]. We call our modified trainable network GroundNet because it empowers ObjectDiffusion to be grounded on the detection layout by mapping the grounding features into the baseline model. GroundNet is connected to the SD baseline via zero-convolution layers [37], implemented as 1×1 zero-initialized convolutional layers. Both the gating mechanism of the GSAs and the zero-convolution layers are important to prevent the noise caused by the new grounding features from damaging the weights of the trainable GroundNet. This is especially important in the initial training phase where noise can harm the pre-training generation knowledge.

ObjectDiffusion is similar to ControlNet in that they both freeze the pretrained SD model and fine-tune a parallel network to adapt to a new control layout. Also, both use zero-convolutional layers to connect the trainable network with the frozen baseline network. However, ObjectDiffusion and ControlNet differ in various aspects. First, ControlNet fine-tunes an exact copy of the locked SD blocks, while ObjectDiffusion modifies the cloned SD blocks with a gated self-attention mechanism which enables the integration of the grounding features. Second, ControlNet adds the extracted condition features to the visual features and injects the concatenated features into the first trainable SD encoder only. In contrast, ObjectDiffusion implements a multi-scale control injection, where the control features are injected into each of the encoder layers and the middle layer of GroundNet. The multi-scale control injection strategy reinforces the control signal and is shown to produce a superior output compared with the standard single injection [75]. Finally, ControlNet processes the control input using an auxiliary convolutional network. Conversely, ObjectDiffusion processes the condition input via CLIP text encoder and Fourier Embedder as laid out in Section 3.2. It is worth noting that the object detection layout presented in Section 3.1 is not among the supported control layouts by the original ControlNet.

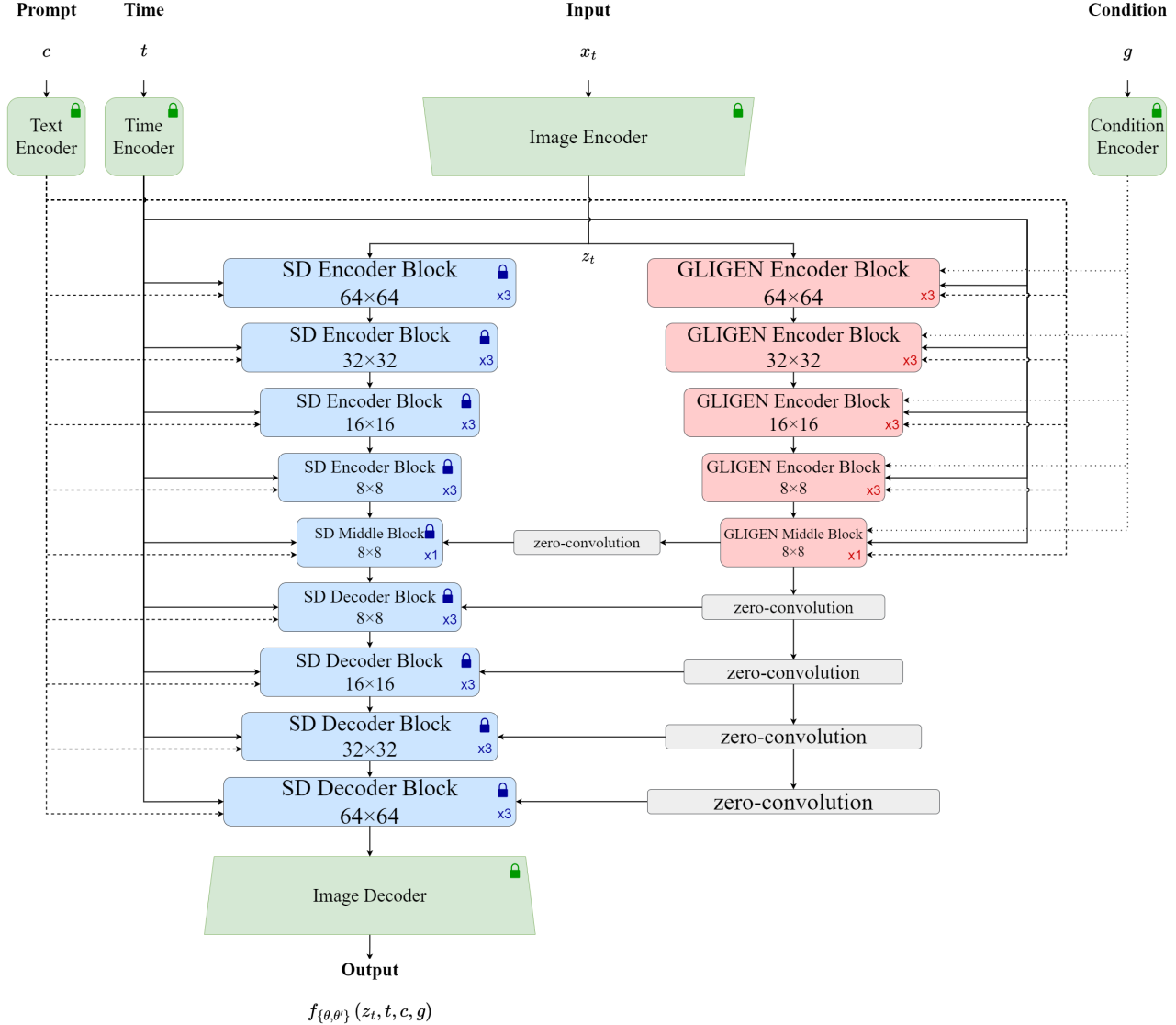


Figure 2. ObjectDiffusion architecture is divided into two parallel networks. First, we utilize Stable Diffusion 1.4v [50] as a pretrained text-to-image model depicted with blue color. The second is a trainable GroundNet which consists of the encoder and middle blocks from GLIGEN [28] represented with red color. GroundNet is capable of processing the conditional layout g which consists of the encoded positional and semantic tokens. During training, both networks receive the time t , the caption c and the image input z_t . The two networks are connected via zero-convolutional layers, highlighted with gray color. ObjectDiffusion operates in latent space. The Image Encoder and Image Decoder project the input image from pixel space to latent space, and the output image from latent space back to pixel space, respectively. Our model architecture design is inspired by ControlNet [73].

3.4. Learning Objective

Diffusion models [58] learn the distribution of the training data by maximizing the log likelihood. Concretely, given a noised version of an image x_t , equivalent to z_t in latent space, and the number of steps t at which the original image x_0 was distorted, a diffusion neural network is trained to predict the amount of noise ϵ added to the image [18]. Accordingly, the training objective is a weighted variational

bound that can be interpreted as a simple L2 loss function between the noise added during the diffusion process and the noise predicted by the model:

$$\min_{\theta} \mathcal{L}_{\text{DM}} = \mathbb{E}_{x,t,\epsilon \sim \mathcal{N}(0,I)} \left[\|\epsilon - f_{\theta}(x_t, t)\|_2^2 \right] \quad (6)$$

where ϵ is the ground-truth noise, θ is the learnable model parameters, and f_{θ} is the predicted noise.

We condition the latent diffusion models $f_{\theta}(z_t, t)$ on

two external inputs, the text caption c and object detection tokens g expressed as:

$$g = [(e_1, b_1), \dots, (e_N, b_N)] \quad (7)$$

where e_i and b_i are the semantic information and the positional information, respectively, corresponding to the i^{th} grounding object.

As discussed in Section 3.3, our proposed framework consists of two networks. The first is a frozen T2I diffusion network $f_\theta(z_t, t, c)$ [50] which conditions the model in text caption c but not in detection tokens g . The second is a trainable GroundNet $f_{\theta'}(z_t, t, c, g)$ which conditions both on caption c and detection tokens g . All components of this module are trainable. The overall noise prediction of our model can be formalized as follows:

$$f_{\{\theta, \theta'\}}(z_t, t, c, g) = f_\theta(z_t, t, c) + Z(f_{\theta'}(z_t, t, c, g)) \quad (8)$$

where Z denotes the zero-convolutional layers. For simplicity, we do not show the weights of Z and assume that the weights of the zero-convolution layers are contained within the weights θ' .

Our learning objective minimizes the L2 loss function that measures the difference between the noise ϵ added to the latent image in the forward process and the noise predicted by the model $f_{\{\theta, \theta'\}}(z_t, t, c, g)$:

$$\min_{\theta'} \mathcal{L} = \mathbb{E}_{z_t, t, c, g, \epsilon \sim \mathcal{N}(0, I)} \left[\|\epsilon - f_{\{\theta, \theta'\}}(z_t, t, c, g)\|_2^2 \right] \quad (9)$$

4. Experiments

4.1. Experimental Setup

Dataset: we fine-tune and evaluate our model on Common Object in Context (COCO) [30] dataset. We use the COCO2017 training split of annotated 118K images for fine-tuning purpose and use the COCO2017 validation split of 5k annotated images for evaluation. The median image ratio is 640×480, and each image in the COCO2017 dataset has 5 captions and an average of 7 objects labels and bounding boxes, classified into 80 simplified categories.

Preprocessing Pipeline: We directly resize with Bicubic [22] interpolation to the desired image size 512×512 pixels, and unlike GLIGEN we do not crop the image at all. The Figure 3 illustrates the difference between our image preprocessing and GLIGEN preprocessing. We randomly flip the image 50% of the time and drop the object grounding annotations when their bounding box area counts for less than 1% of the image area. Additionally, we only keep the 30 objects that have the largest areas. The bounding boxes are converted from COCO format $[x_{min}, y_{min}, w, h]$ to the format $[x_{min}, y_{min}, x_{max}, y_{max}]$.

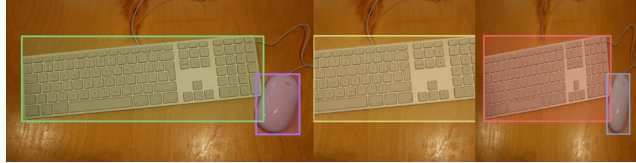


Figure 3. The original image is to the left, GLIGEN [28] preprocessed image is in the middle, and our preprocessing image is to the right. This figure highlights the difference between the resizing via the Bicubic [22] interpolation that we apply and the center cropping implemented in GLIGEN.

Initialization: Initializing our model weights from pretrained models enables us to capitalize on and build upon the extensive knowledge acquired through prior training. We initialize the text-to-image model using Stable-Diffusion-v-1-4 [7] due to its compatibility with GLIGEN which allows for a fair comparison to the SOTA model. Stable-Diffusion-v-1-4 is extensively trained on high-resolution subset of the large-scale LAION-5B [54] dataset. We initialize GroundNet from GLIGEN’s diffusers-generation-text-box checkpoint [13] which is pretrained on manually annotated object names and bounding boxes from the Object365 [56], Flickr [42] and Visual Genome (VG) [25] datasets in addition to object names and bounding boxes extracted via GLIP [26] from the SBU [39], and CC3M [57] datasets but with no fine-tuning on the COCO [30] dataset. We freeze the pretrained CLIP ViT-L/14 [46] text encoder during the whole training process. ObjectDiffusion contains 1.32 billion parameters, 460.8M of them are trainable parameters and 860M frozen parameters.

Implementation Details: We fine-tune ObjectDiffusion for 100k iterations with a learning rate 5×10^{-5} on a single NVIDIA QUADRO GV100 32 GB GPU using Adam [23] optimizer. We set the warmup iterations to 4k and apply no weight decay. We randomly choose 1 out of the 5 available COCO captions. To ensure that the training is robust, we randomly drop the caption and randomly drop the condition input, each with a 10% independent probability.

We utilize some techniques to overcome the limitations in GPU memory and computational capacity. First, we implement the Automatic Mixed Precision (AMP) [33], a smart quantization technique that assigns multiple precisions to different modules of the same model according to their tolerance of low precision. AMP delivers a 109% speedup in training. Second, we employ Gradient Accumulation [24], that is, we train with a batch size of 4 but update the model weights with the normalized accumulated gradients once every 4 iterations. Gradient Accumulation allows us to quadruple the batch size from 4 to 16 which smooths the learning curve.

Evaluation Benchmarks: We use the COCO2017 evaluation set to quantitatively and qualitatively assess Object-

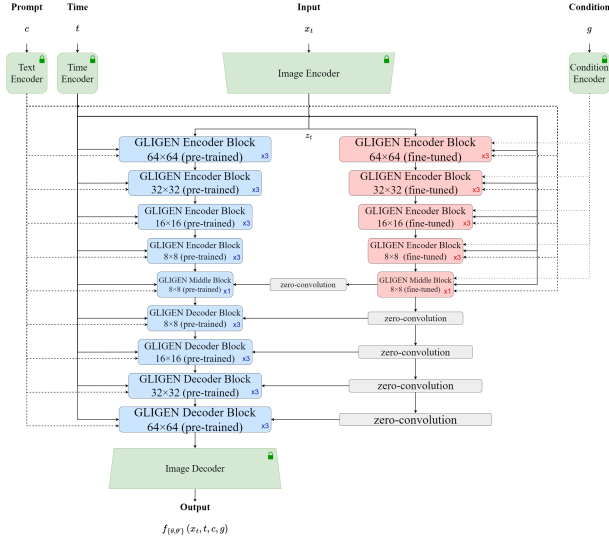


Figure 4. The inference schema consists of our GroundNet fine-tuned on COCO2017 [30] object detection annotations. GroundNet is displayed in red color. The second part is a full pretrained GLIGEN [28] network showed in blue color. We replace the pretrained Stable Diffusion [50] model that we used in training with pretrained GLIGEN [28] because it yields more precise grounding abilities. GLIGEN [28] is trained on Object365 [56], GoldG [26] (Flickr and VG), SBU [39], and CC3M [57] datasets but not on COCO [30] dataset.

Diffusion on closed-set setting. Specifically, we calculate the Average Precision (AP) [40] and the Average Recall (AR) [40] on 5k generated images using a YOLOv8m [49] pretrained model to measure the precision of our model in rendering the correct objects in the intended locations. We quantify the image quality by generating 20k images and computing the Fréchet Inception Distance (FID) [17] score between the generated images and the real images. For open-set assessment, we craft image captions and grounding inputs and qualitatively analyze the output visuals.

Inference: During inference, we keep the fine-tuned GroundNet and replace the SD model with a full pretrained GLIGEN network, as we have empirically verified that GLIGEN yields more controllable images. The inference model architecture is depicted in Figure 4. In all of our experiments, we sample 512×512 RGB images using Pseudo Linear Multi-Step (PLMS) [31] sampler with a guidance scale of 7.5 and 50 steps.

4.2. Quantitative Results

Table 1 details the Average Precision (AP, AP₅₀, AP₇₅) [40] metrics and Average Recall (AR) [40] metric between the YOLOv8m [49] predictions and ground truth attributes. ObjectDiffusion achieves 27.4, 46.6 28.2, and 44.5 in AP, AP₅₀, AP₇₅, and AR, respectively.

Our model surpasses the state-of-the-art model [28] in AP₅₀ score by more than 10% and obtains competitive AP and AP₇₅ scores surpassing most of the layout-to-image models including LostGAN-V2 [62], LAMA [29], TwFA [71], and GLIGEN [28]. Our high AP scores indicate that ObjectDiffusion succeeded in learning from ground information and was able to synthesize images in a high alignment with the control input. Our model was able to increase the zero-shot AP score of GLIGEN (zero-shot) from 19.1 to 27.4 and the score of the AP₅₀ from 30.5 to 46.6 which indicates a successful training on the COCO2017 [30] dataset. The results also show that our approach circumvents the problem of “knowledge forgetting” that typically hinders fine-tuning layout-to-image models.

In Table 2 we calculate the AP and AP₅₀ score values per class and report the first three classes with the highest AP values and the first three classes with the lowest AP values. The classes “cat”, “bear”, and “dog” are the top classes where our model was able to ground with a very high precision. On the other hand, “book”, “hair drier”, and “sports ball” are the classes that confound our model the most. Unexpectedly, the effectiveness of grounding an object category does not correlate with the category frequency in the dataset. For example, the category “book” is overrepresented in the COCO2017 dataset, however it has a very low AP value. Similarly, the “cat”, “dog”, and bear categories are underrepresented in the COCO2017 dataset, but they have the highest AP values.

Table 3 shows that our model achieves the highest reported AR score 44.5 only 5 points behind the upper bound value. The high AR value suggests that ObjectDiffusion rarely overlooks objects which is a common issue that text-to-image models suffer from.

Finally, to measure the quality of our model generation, we calculate the FID [17] scores in Table 4. ObjectDiffusion achieves a FID score of 19.8 outperforming the state-of-the-art model GLIGEN (fine-tuned), GLIGEN, and the GLIGEN (zero-shot) by 6%, 8% and 27%, respectively. The improvement in FID score proves the efficiency of our proposed training architecture in learning the generation capabilities for high-quality image synthesis.

It’s worth noting that our evaluation is limited to models trained on publicly available datasets.

4.3. Qualitative Results

We visually demonstrate the capabilities of ObjectDiffusion to ground on boxes and entities. We test our model under both closed-set vocabulary entity names and open-set vocabulary entity names. Our qualitative testing is designed to encompass various entities such as animals, persons, vehicles, home stuffs, and sports in indoors and outdoors contexts. To verify our model ability to generate satisfactory images from challenging requirements we vary the bound-

Model	YOLOv8m [49]		
	AP (↑)	AP ₅₀ (↑)	AP ₇₅ (↑)
upper-bound	49.7	65.5	-
LostGAN-V2 [62]	9.1	15.3	9.8
LAMA [29]	13.40	19.70	14.90
TwFA [71]	-	28.20	20.12
GLIGEN [28]	22.4	36.5	24.1
pretrained on (Object365, GoldG, SBU, CC3M)			
GLIGEN (zero-shot) [28]	19.1	30.5	20.8
GLIGEN (fine-tuned) [28]	30.8	42.3	35.3
ObjectDiffusion (ours)	27.4	46.6	28.2

Table 1. Evaluation of grounding precision on synthesized images is generated using the captions, boxes, and instance classes from COCO2017 [30] validation set. The AP, AP₅₀ and AP₇₅ metrics [40] of ObjectDiffusion and the upper-bound are calculated using a pretrained YOLOv8m [49] object detection model on image size 512×512. Other numbers are taken from [28].

	Class	YOLOv8m [49]	
		AP (↑)	AP ₅₀ (↑)
Highest AP Classes	cat	74.2	96.7
	bear	70.3	91.0
	dog	62.7	87.5
Lowest AP Classes	book	4.6	11.0
	hair drier	4.3	6.1
	sports ball	3.7	10.9

Table 2. This table lists COCO [30] classes with the highest AP scores (cat, bear, dog) and COCO classes with the lowest AP [40] scores (book, hair drier, sports ball). Values are calculated using YOLOv8m [49] object detection model on images synthesized from COCO2017 validation set annotations with image size 512×512.

ing box sizes, the bounding box locations, the number of objects per image, and the length of object names.

Closed-set Setting Evaluation: Figures 6 to 10 display representative images under closed-set vocabulary setting. All closed-set images are synthesized with COCO2017 validation set annotations. Each figure showcases a specific general concept like people, animals, vehicles, and rooms.

Figure 6 various photo-realistic locations from a standard home showing the ability of ObjectDiffusion to synthesize high-quality, precise images from complex layouts. For example, the layout of the image (c) in the first row of Figure 6 is an object-intense visual of living room furniture. That is, the layout contains 19 size-varying bounding boxes labeled with 8 entity classes such as “couch”, “chair”, “vase”, and “tv”.

Figure 7 shows a collection of land vehicles, railway vehicles, and watercraft. The second row of Figure 7 demonstrates our model’s capabilities in adapting to bounding boxes with varying aspect ratios. ObjectDiffusion successfully accommodated the “motorcycles” and the “persons” in each of the three instances in respect to the grounding

entity locations and sizes. Additionally, the output images adhered to the image caption, that is, placing the “motorcycle” on a paved track in the left image, on a dirt track in the middle image, and on a highway in the right image.

In Figure 8 we list some synthesized images of people in formal and casual situations. ObjectDiffusion renders photo-realistic portraits with authentic facial appearance. We notice that in image (c) of Figure 8 the man is wearing sunglasses but is missing the black hat specified in the prompt. We think that the model may not have seen enough suit wearing men with hats on their heads. We also notice, in the same image, that the “tie” is not 100% positioned within the box boundaries. We also observe that the hands of people in the (b) and (c) images are not perfect. These constraints are inherited from the pretrained text-to-image model weights that we initialized our model from.

We exhibit instances of domestic and wild animals in Figure 9 where we demonstrate artificial images of dogs, cats, horses, and bears. The high grounding precision of qualitative examples of different kinds of animals are in line with the high AP scores obtained in animal categories reported in Table 2.

The last examples of visuals generated under closed-set vocabulary settings are collected in Figure 10. This figure depicts images of teddy bears, vases, food, and sport activities.

ObjectDiffusion can ground instances from a single grounding box or multiple grounding boxes, like in the “teddy bear” instances. We can utilize image prompt as a global condition that describes the overall surroundings and background. For example, the images (b) and (c) in Figure 10 show a “teddy bear” laying on a wall and “teddy bears” sitting on a sofa. In some cases, our model may overlook the colors or the materials of the conditional objects, like the color of the “vase” in image (f). ObjectDiffusion grounding ability is not limited to static objects. The last row of Figure 10 illustrates that our model can actually render objects

in dynamic moving scenes like skiing and surfing in (j), (k) and (l) examples.

Open-set Setting Evaluation: We evaluate ObjectDiffusion performance in grounding the generation process on entity names that are not present in training data. To do so, we manually craft the caption, regional, and semantic grounding inputs using instance names outside the 80 COCO2017 classes. In Figure 11 we provide three examples per annotation.

The first row (a) demonstrates image examples of a modern house in Scandinavian style. We can use the category names from the 80 COCO categories but with modifier attributes preceding the name, such as a “comfy couch”, a “stylish coffee table” or can use completely new concepts, such as “sunlit windows”. We observe a noticeable improvement in quality in the open-set settings compared to their closed-set. This enhancement may be explained by the flexibility that the open-ended text form can provide.

Second row (b) depicts visuals of fancy desk setups. ObjectDiffusion can understand long and complex captions and entity texts such as “a sleek, ultra-thin, high resolution bezel-less monitor”. Our model was creative in rendering the three “vases”, each with a distinct shape.

Third row (c) contains stunning images of a modern high speed train passing beside a majestic waterfall. Even though the “waterfall” is an uncommon object and has never been seen as an instance name in COCO2017 dataset, our model was able to interpret and handle it. However, we observe that all of our output images in the middle row missed the “tunnel”. This maybe because it was not in the grounding entity input. The open-set qualitative visuals indicate that ObjectDiffusion was able to retain the knowledge of the pretrained text-to-image model while successfully demonstrating the conditioning abilities from the weights of the pretraining and the fine-tuning grounding task.

Model	YOLOv8m [49] AR (↑)
upper-bound	49.7
GLIGEN [28]	30.7
ObjectDiffusion (ours)	44.5

Table 3. This table represents the evaluation of ObjectDiffusion ability to correctly render objects specified in condition layout. ObjectDiffusion shows an outstanding ability of generating the prescribed entities and overcoming the “overlooking problem” that some text-to-image and layout-to-image models suffer from. The AR [40] score of ObjectDiffusion and upper-bound is calculated using a pretrained YOLOv8m [49] object detection model on synthesized images from the COCO2017 [30] validation set annotations with image size 512×512. Other numbers are taken from [28].

The last row (d) in Figure 11 emphasizes the powerful

regional grounding skills of our model. The layout is constructed by stacking three bounding boxes of varying sizes belonging to the same object name, “a fluffy Pomeranian”. As seen by synthesized images, ObjectDiffusion succeeds in generating the correct entity with the correct size in the correct location. Furthermore, our model exhibits high level of diversity, that is, it renders the “Pomeranians” with three different colors, brown, white, and black, and with three different background illumination contrasts.

Examples of the open-set images demonstrate ObjectDiffusion capabilities of synthesizing realistic and artistic visuals, both of which are spectacular, diverse, and high-quality.

4.4. Limitations and Failures

ObjectDiffusion is able to synthesize high quality scenes, however sometimes struggles in capturing the intricate fine-grained details of faces, hands, and feet [51]. Faces are highly detailed, complex structures that exhibit a high degree of variability. Image (a) in Figure 5 is an example of a young man with distorted face and hands.

Similar to the limitation in face synthesis, ObjectDiffusion manifests an imperfection in rendering images that contains text. We notice that our model repeatedly failed in rendering these images, even though our fine-tuning dataset contains an abundance of images featuring the embedded text. We can notice from the image (b) in Figure 5 our model failed in overlaying a short single-word text on the stop sign.

ObjectDiffusion may overly attend to the control signals, that is, the bounding boxes, which may lead to an unconventional placement of entities. For example, the image (c) in Figure 5 shows a “dog” sitting on top of a “vehicle”. While the objects are rendered in the correct regions specified via the bounding boxes, the legs of the “dog” are not touching the “truck”, resulting in an absurd scene.

5. Discussion and Conclusion

In this work, we have taken inspiration from the two prominent works, ControlNet and GILGEN to propose a new model ObjectDiffusion. Our model learns to ground T2I models on entity name and bounding box annotations. ObjectDiffusion exceeds the current state-of-the-art GLIGEN (fine-tuned) trained on open-source datasets in AP₅₀ and AR metrics. Our model also scores higher than the top-scoring layout-to-image baselines. In the FID quality metric, our model surpasses the top scores of both specialized layout-to-image and diffusion-based models conditioned on COCO2017 object detection annotations. Qualitative evaluation demonstrates the ability of ObjectDiffusion to synthesize diverse high-quality, high-fidelity images that seamlessly adhere to the conditional inputs.



Figure 5. This figure showcases some limitations of our model in generating faces and hands of people as shown in image (a). It also highlights the limitations of rendering legible, correct text as in image (b). ObjectDiffusion may synthesize images that precisely adhere to the conditional bounding boxes but have irrational position alignments and interactions between objects, for example, in image (c) the “dog” is absurdly floating above the “truck”. The images are generated using grounding entities and image captions from COCO2017 [30] validation set.

Model	FID (↓)
LostGAN-V2 [62]	42.55
OCGAN [63]	41.65
HCSS [21]	33.68
LAMA [29]	31.12
TwFA [71]	22.15
GLIGEN [28]	21.04
pretrained on (Object365, GoldG, SBU, CC3M)	
GLIGEN (zero-shot) [28]	27.03
GLIGEN (fine-tuned) [28]	21.58
ObjectDiffusion (ours)	19.80

Table 4. This table lists the quality evaluation results of generated images from COCO2017 [30] validation set. We use FID [17] score implementation from [55] and resize the real and generated images to 299×299 before calculating the FID score. Other FID scores are taken from [28].

While ObjectDiffusion has demonstrated a remarkable performance, several improvements may further enhance the model’s capabilities. First, training on a large-scale dataset that contains precise and detailed entity names could bring a significant increase in AP score. Second, further training our model may lead to a pronounced gain in the overall performance. Additionally, training on powerful GPUs would enable fitting a larger batch size of 32 or 64 and allows the use of full float32 precision. While we achieve a remarkable improvement, scaling up the training has the potential to accelerate the model convergence and further improve the generation precision and quality.

Acknowledgment

We are deeply grateful to Thomas J. Crabtree for his valuable assistance with language editing and spelling corrections.

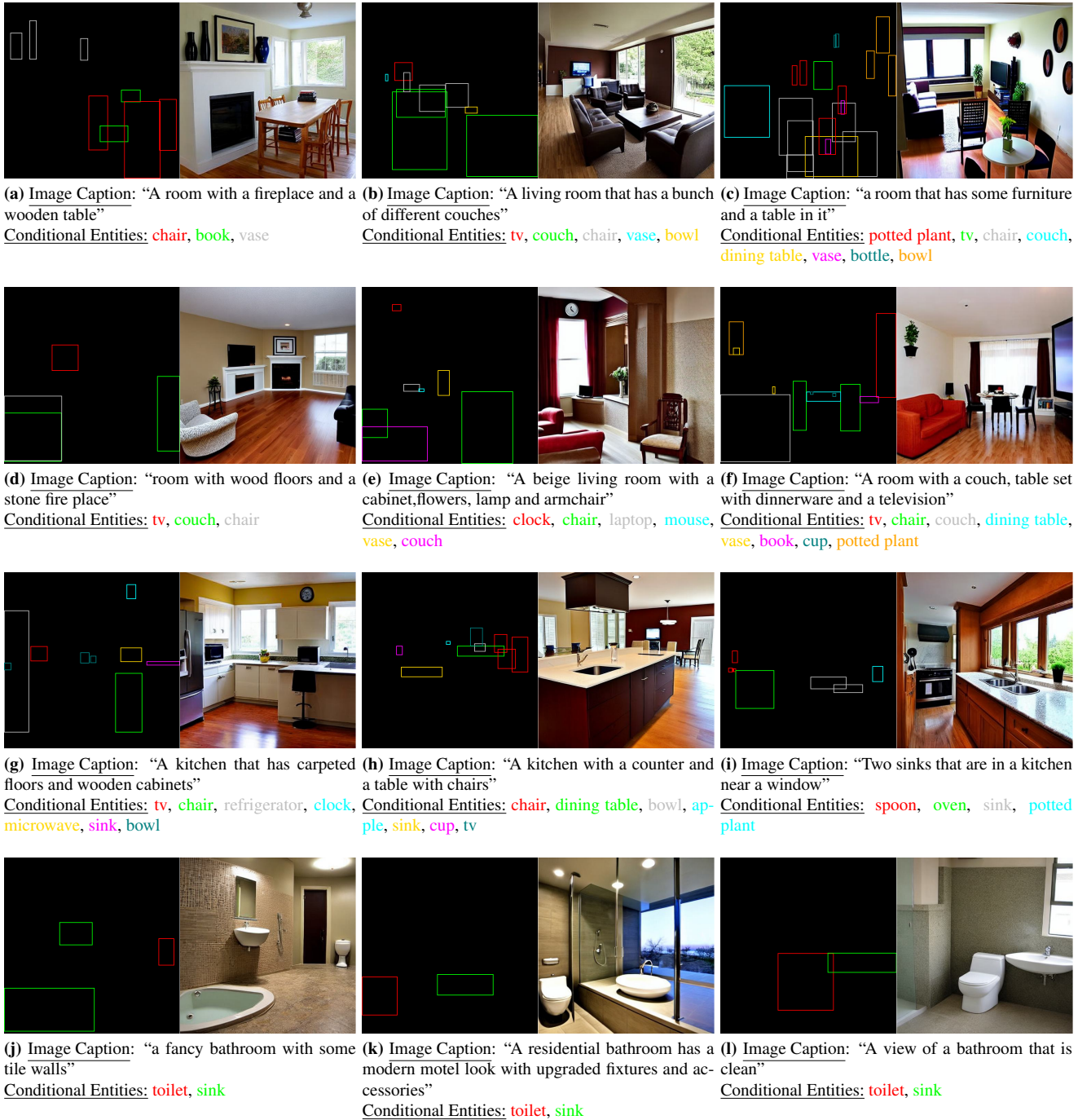


Figure 6. This figure represents qualitative examples of closed-set configuration. Images are generated from COCO2017 [30] validation set annotations. Our model demonstrates precise generation capabilities of complex indoor visuals, for example, living rooms, kitchens, and bathrooms.

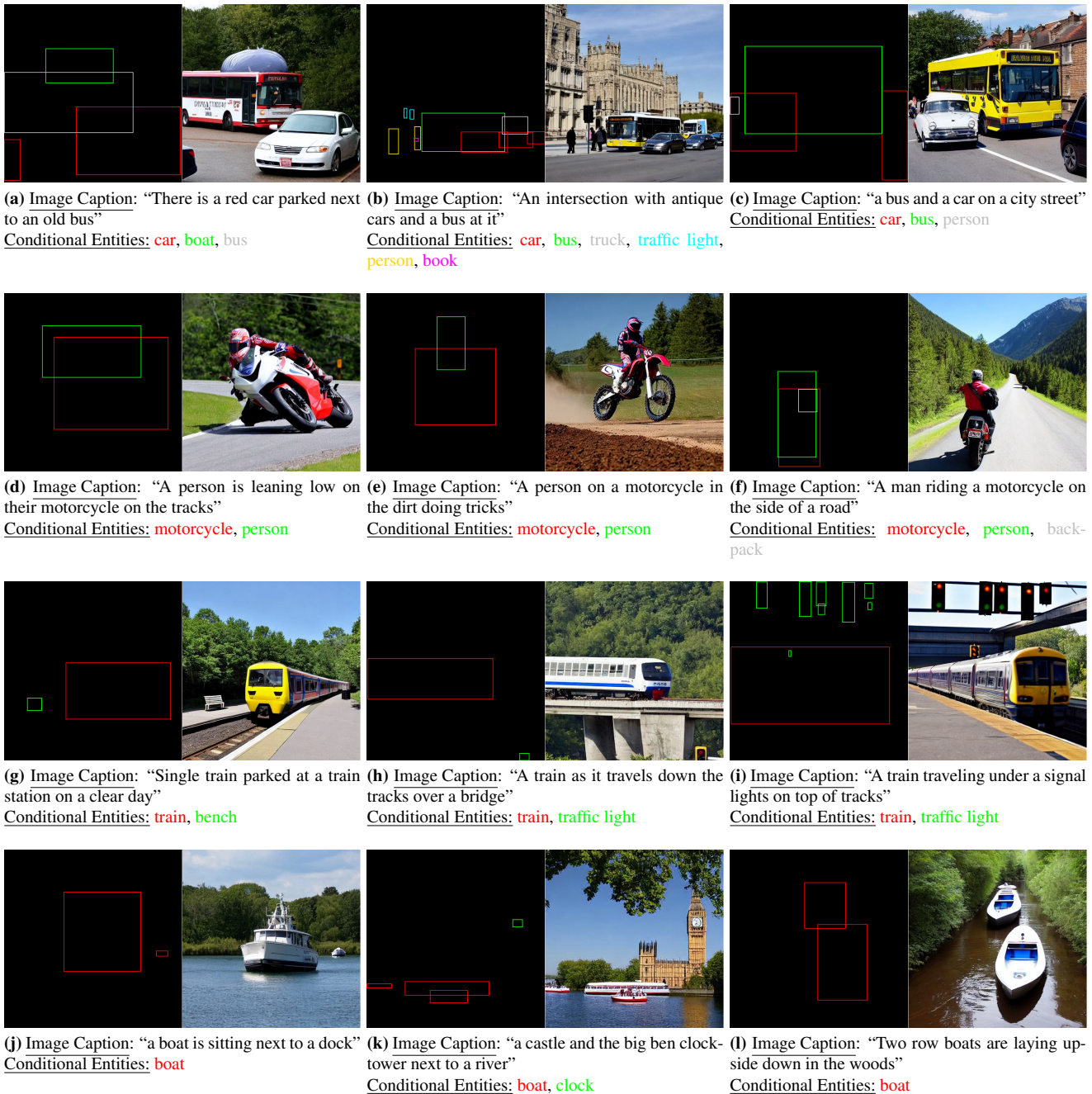


Figure 7. This figure represents qualitative examples of closed-set configuration. Images are generated using grounding entities and image captions from COCO2017 [30] validation set annotations. Our framework can accurately render different classes of vehicles like cars, trains, motorcycles, and boats.

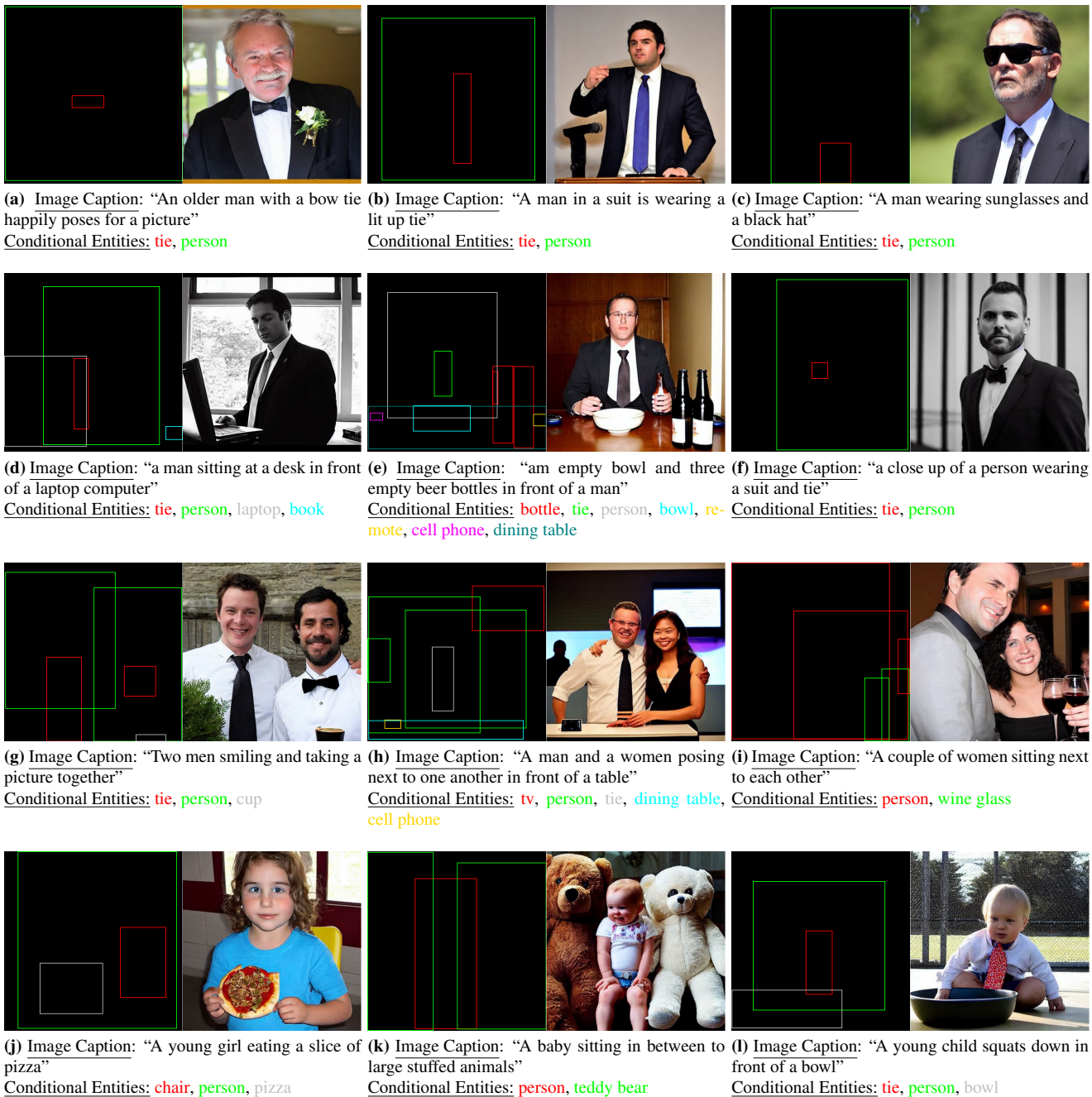


Figure 8. This figure represents qualitative examples of closed-set configuration. Images are generated using grounding entities and image captions from COCO2017 [30] validation set annotations. The portraits generated by ObjectDiffusion feature realistic facial expressions.

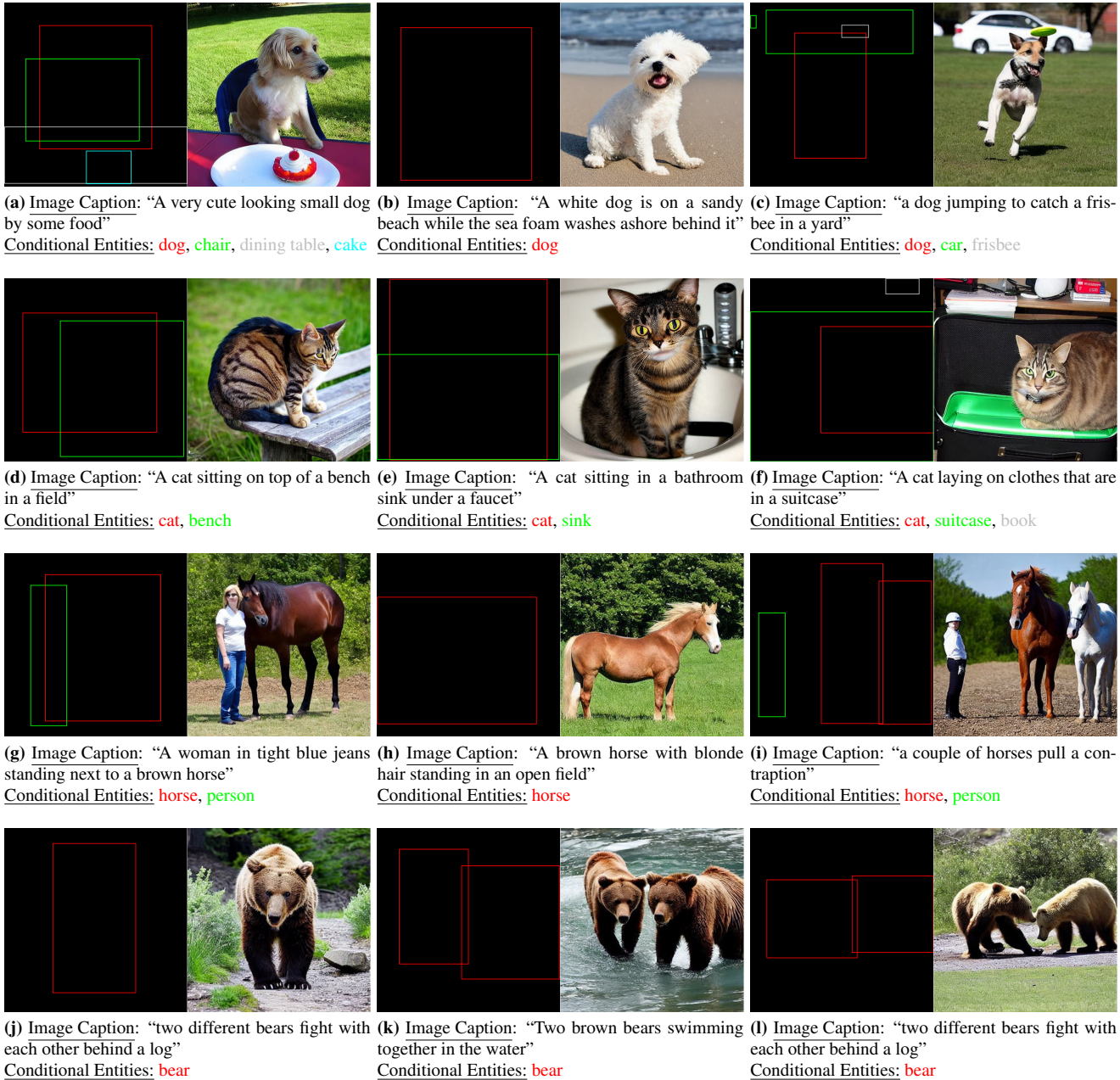


Figure 9. This figure represents qualitative examples of closed-set configuration. Images are generated using grounding entities and image captions from COCO2017 [30] validation set annotations. Our framework achieves proficiency in generating high-resolution visuals of animals in their native habitat with a very high AP precision score.

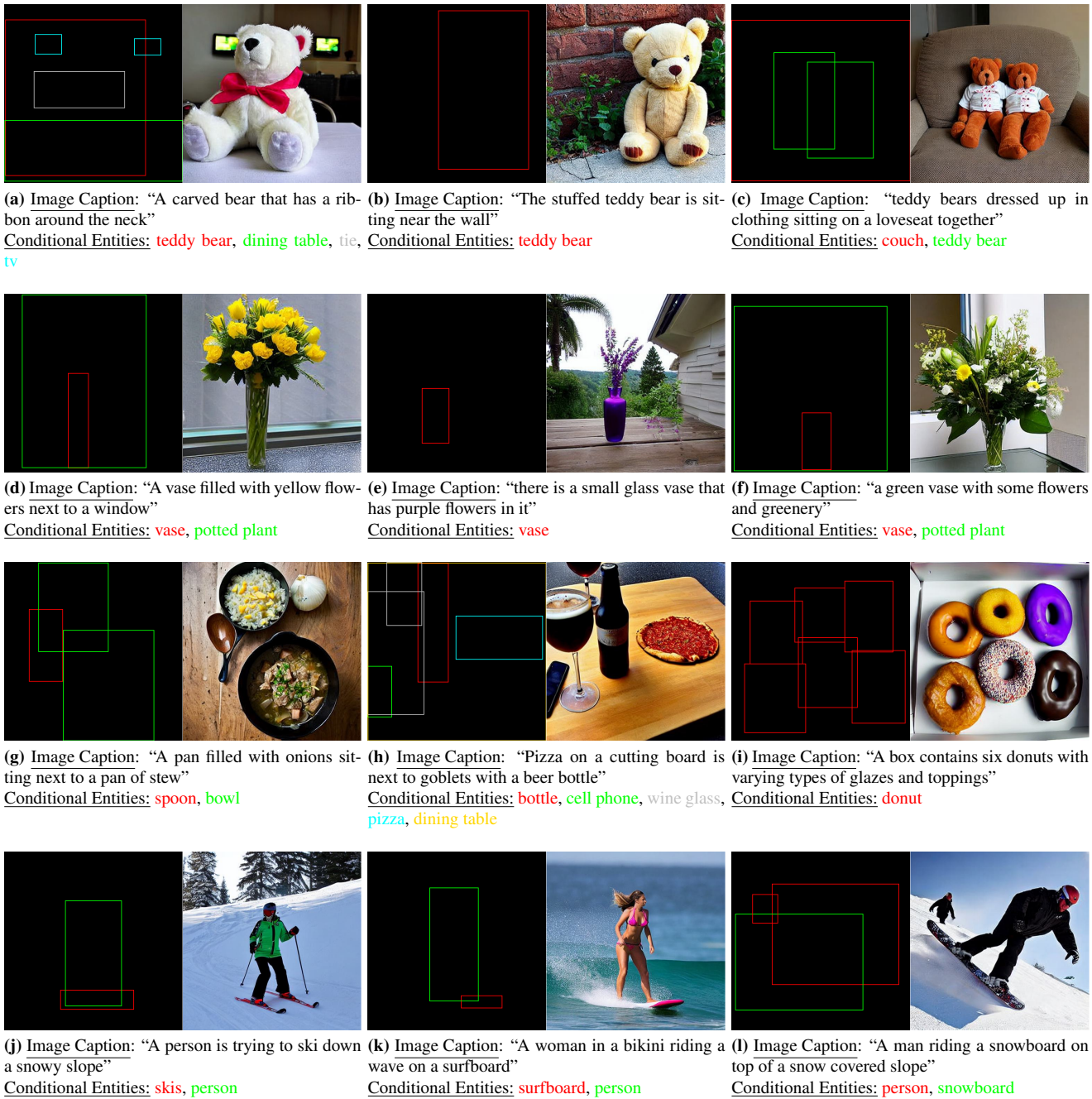


Figure 10. This figure represents qualitative examples of closed-set configuration. Images are generated using grounding entities and image captions from COCO2017 [30] validation set annotations. This figure shows static and dynamic scenes of different object categories. ObjectDiffusion can synthesize images of dishes and visuals of sport activities, for example, surfing and skiing



(a) Image Caption: “bright modern Scandinavian style house with a comfy couch, stylish coffee table, and sunlit windows homevibes relaxation”
 Conditional Entities: a comfy couch, a stylish coffee table, a sunlit windows



(b) Image Caption: “a sleek, ultra-thin, high resolution bezel-less monitor, realistic, modern, detailed, vibrant colors, glossy finish, floating design, lowlight, art by peter mohrbacher and donato giancola, digital illustration, trending on Artstation, high-tech, smooth, minimalist workstation background, crisp reflection on screen, soft lighting”
 Conditional Entities: a sleek, ultra-thin, high resolution bezel-less monitor, a keyboard, a mouse, a studying desk, a vase, a window



(c) Image Caption: “a waterfall and a modern high speed train running through the tunnel in a beautiful forest with fall foliage”
 Conditional Entities: a waterfall, a modern high speed train



(d) Image Caption: “a beautiful digital painting depicting fluffy Pomeranian in a green forest, impressionism painting style, impressive, masterpiece”
 Conditional Entities: a fluffy Pomeranian

Figure 11. This figure represents realistic and artistic qualitative examples of open-set configuration with manual annotations.

References

- [1] Midjourney. <https://www.midjourney.com>, 2023. (accessed 15 July 2024). 1
- [2] Jean-Baptiste Alayrac, Jeff Donahue, Pauline Luc, Antoine Miech, Iain Barr, Yana Hasson, Karel Lenc, Arthur Mensch, Katherine Millican, Malcolm Reynolds, et al. Flamingo: a visual language model for few-shot learning. *Advances in neural information processing systems*, 35:23716–23736, 2022. 4
- [3] Arpit Bansal, Hong-Min Chu, Avi Schwarzschild, Soumyadip Sengupta, Micah Goldblum, Jonas Geiping, and Tom Goldstein. Universal guidance for diffusion models. In *Proceedings of the IEEE/CVF Conference on Computer Vision and Pattern Recognition*, pages 843–852, 2023. 3
- [4] John Canny. A computational approach to edge detection. *IEEE Transactions on pattern analysis and machine intelligence*, (6):679–698, 1986. 1, 2
- [5] Zhe Cao, Tomas Simon, Shih-En Wei, and Yaser Sheikh. Realtime multi-person 2d pose estimation using part affinity fields. In *Proceedings of the IEEE conference on computer vision and pattern recognition*, pages 7291–7299, 2017. 1, 2
- [6] Minghao Chen, Iro Laina, and Andrea Vedaldi. Training-free layout control with cross-attention guidance. In *Proceedings of the IEEE/CVF Winter Conference on Applications of Computer Vision*, pages 5343–5353, 2024. 3
- [7] CompVis. <https://huggingface.co/CompVis/stable-diffusion-v-1-4-original>, 2023. Hugging Face, (accessed 27 January 2024). 6
- [8] Prafulla Dhariwal and Alexander Nichol. Diffusion models beat gans on image synthesis. *Advances in neural information processing systems*, 34:8780–8794, 2021. 2
- [9] Shiv Ram Dubey, Satish Kumar Singh, and Bidyut Baran Chaudhuri. Activation functions in deep learning: A comprehensive survey and benchmark. *Neurocomputing*, 503: 92–108, 2022. 4
- [10] Stefan Elfving, Eiji Uchibe, and Kenji Doya. Sigmoid-weighted linear units for neural network function approximation in reinforcement learning. *Neural networks*, 107:3–11, 2018. 4
- [11] Wan-Cyuan Fan, Yen-Chun Chen, DongDong Chen, Yu Cheng, Lu Yuan, and Yu-Chiang Frank Wang. Frido: Feature pyramid diffusion for complex scene image synthesis. In *Proceedings of the AAAI conference on artificial intelligence*, pages 579–587, 2023. 3
- [12] Stanislav Frolov, Avneesh Sharma, Jörn Hees, Tushar Karayil, Federico Raue, and Andreas Dengel. Attrlostgan: Attribute controlled image synthesis from reconfigurable layout and style. In *DAGM German Conference on Pattern Recognition*, pages 361–375. Springer, 2021. 3
- [13] gligen. <https://https://huggingface.co/gligen/diffusers-generation-text-box>, 2023. Hugging Face, (accessed 2 February 2024). 6
- [14] Ian Goodfellow, Jean Pouget-Abadie, Mehdi Mirza, Bing Xu, David Warde-Farley, Sherjil Ozair, Aaron Courville, and Yoshua Bengio. Generative adversarial nets. *Advances in neural information processing systems*, 27, 2014. 1, 2
- [15] Geonmo Gu, Byungsoo Ko, SeoungHyun Go, Sung-Hyun Lee, Jingeun Lee, and Minchul Shin. Towards light-weight and real-time line segment detection. In *Proceedings of the AAAI Conference on Artificial Intelligence*, pages 726–734, 2022. 2
- [16] David Ha, Andrew Dai, and Quoc V Le. Hypernetworks. *arXiv preprint arXiv:1609.09106*, 2016. 3
- [17] Martin Heusel, Hubert Ramsauer, Thomas Unterthiner, Bernhard Nessler, and Sepp Hochreiter. Gans trained by a two time-scale update rule converge to a local nash equilibrium. *Advances in neural information processing systems*, 30, 2017. 2, 7, 10
- [18] Jonathan Ho, Ajay Jain, and Pieter Abbeel. Denoising diffusion probabilistic models. *Advances in neural information processing systems*, 33:6840–6851, 2020. 5
- [19] Neil Houlsby, Andrei Giurgiu, Stanislaw Jastrzebski, Bruna Morrone, Quentin De Laroussilhe, Andrea Gesmundo, Mona Attariyan, and Sylvain Gelly. Parameter-efficient transfer learning for nlp. In *International conference on machine learning*, pages 2790–2799. PMLR, 2019. 2
- [20] Edward J Hu, Yelong Shen, Phillip Wallis, Zeyuan Allen-Zhu, Yuanzhi Li, Shean Wang, Lu Wang, and Weizhu Chen. Lora: Low-rank adaptation of large language models. *arXiv preprint arXiv:2106.09685*, 2021. 2
- [21] Manuel Jahn, Robin Rombach, and Björn Ommer. High-resolution complex scene synthesis with transformers. *arXiv preprint arXiv:2105.06458*, 2021. 2, 10
- [22] Robert Keys. Cubic convolution interpolation for digital image processing. *IEEE transactions on acoustics, speech, and signal processing*, 29(6):1153–1160, 1981. 6
- [23] Diederik P Kingma. Adam: A method for stochastic optimization. *arXiv preprint arXiv:1412.6980*, 2014. 6
- [24] Nikita Kozodoi. Gradient accumulation in pytorch. <https://kozodoi.me/blog/20210219/gradient-accumulation>, 2021. (accessed 7 February 2024). 6
- [25] Ranjay Krishna, Yuke Zhu, Oliver Groth, Justin Johnson, Kenji Hata, Joshua Kravitz, Stephanie Chen, Yannis Kalantidis, Li-Jia Li, David A Shamma, et al. Visual genome: Connecting language and vision using crowdsourced dense image annotations. *International journal of computer vision*, 123:32–73, 2017. 6
- [26] Liunian Harold Li, Pengchuan Zhang, Haotian Zhang, Jianwei Yang, Chunyuan Li, Yiwu Zhong, Lijuan Wang, Lu Yuan, Lei Zhang, Jenq-Neng Hwang, et al. Grounded language-image pre-training. In *Proceedings of the IEEE/CVF Conference on Computer Vision and Pattern Recognition*, pages 10965–10975, 2022. 2, 6, 7
- [27] Yandong Li, Yu Cheng, Zhe Gan, Licheng Yu, Liqiang Wang, and Jingjing Liu. Bachgan: High-resolution image synthesis from salient object layout. In *Proceedings of the IEEE/CVF Conference on Computer Vision and Pattern Recognition*, pages 8365–8374, 2020. 3
- [28] Yuheng Li, Haotian Liu, Qingyang Wu, Fangzhou Mu, Jianwei Yang, Jianfeng Gao, Chunyuan Li, and Yong Jae Lee. Gligen: Open-set grounded text-to-image generation. In *Proceedings of the IEEE/CVF Conference on Computer Vision and Pattern Recognition*, pages 22511–22521, 2023. 2, 3, 4, 5, 6, 7, 8, 9, 10

- [29] Zejian Li, Jingyu Wu, Immanuel Koh, Yongchuan Tang, and Lingyun Sun. Image synthesis from layout with locality-aware mask adaptation. In *Proceedings of the IEEE/CVF International Conference on Computer Vision*, pages 13819–13828, 2021. [2](#), [3](#), [7](#), [8](#), [10](#)
- [30] Tsung-Yi Lin, Michael Maire, Serge Belongie, James Hays, Pietro Perona, Deva Ramanan, Piotr Dollár, and C Lawrence Zitnick. Microsoft coco: Common objects in context. In *Computer Vision—ECCV 2014: 13th European Conference, Zurich, Switzerland, September 6–12, 2014, Proceedings, Part V 13*, pages 740–755. Springer, 2014. [2](#), [3](#), [6](#), [7](#), [8](#), [9](#), [10](#), [11](#), [12](#), [13](#), [14](#), [15](#)
- [31] Luping Liu, Yi Ren, Zhijie Lin, and Zhou Zhao. Pseudo numerical methods for diffusion models on manifolds. *arXiv preprint arXiv:2202.09778*, 2022. [7](#)
- [32] Vivian Liu and Lydia B Chilton. Design guidelines for prompt engineering text-to-image generative models. In *Proceedings of the 2022 CHI conference on human factors in computing systems*, pages 1–23, 2022. [1](#)
- [33] Paulius Micikevicius, Sharan Narang, Jonah Alben, Gregory Diamos, Erich Elsen, David Garcia, Boris Ginsburg, Michael Houston, Oleksii Kuchaiev, Ganesh Venkatesh, et al. Mixed precision training. *arXiv preprint arXiv:1710.03740*, 2017. [6](#)
- [34] B Mildenhall, PP Srinivasan, M Tancik, JT Barron, R Ramamoorthi, and R Ng Nerf. Representing scenes as neural radiance fields for view synthesis., 2021, 65. DOI: <https://doi.org/10.1145/3503250>, pages 99–106. [3](#), [4](#)
- [35] Chong Mou, Xintao Wang, Liangbin Xie, Yanze Wu, Jian Zhang, Zhongang Qi, and Ying Shan. T2i-adapter: Learning adapters to dig out more controllable ability for text-to-image diffusion models. In *Proceedings of the AAAI Conference on Artificial Intelligence*, pages 4296–4304, 2024. [2](#)
- [36] Alex Nichol, Prafulla Dhariwal, Aditya Ramesh, Pranav Shyam, Pamela Mishkin, Bob McGrew, Ilya Sutskever, and Mark Chen. Glide: Towards photorealistic image generation and editing with text-guided diffusion models. *arXiv preprint arXiv:2112.10741*, 2021. [1](#)
- [37] Alexander Quinn Nichol and Prafulla Dhariwal. Improved denoising diffusion probabilistic models. In *International conference on machine learning*, pages 8162–8171. PMLR, 2021. [4](#)
- [38] OpenAI. Dall-e-2. <https://openai.com/product/dall-e-2>, 2023. (accessed 4 May 2024). [1](#)
- [39] Vicente Ordonez, Girish Kulkarni, and Tamara Berg. Im2text: Describing images using 1 million captioned photographs. *Advances in neural information processing systems*, 24, 2011. [2](#), [6](#), [7](#)
- [40] Rafael Padilla, Sergio L Netto, and Eduardo AB Da Silva. A survey on performance metrics for object-detection algorithms. In *2020 international conference on systems, signals and image processing (IWSSIP)*, pages 237–242. IEEE, 2020. [7](#), [8](#), [9](#)
- [41] Nikita Pavlichenko and Dmitry Ustalov. Best prompts for text-to-image models and how to find them. In *Proceedings of the 46th International ACM SIGIR Conference on Research and Development in Information Retrieval*, pages 2067–2071, 2023. [1](#)
- [42] Bryan A Plummer, Liwei Wang, Chris M Cervantes, Juan C Caicedo, Julia Hockenmaier, and Svetlana Lazebnik. Flickr30k entities: Collecting region-to-phrase correspondences for richer image-to-sentence models. In *Proceedings of the IEEE international conference on computer vision*, pages 2641–2649, 2015. [6](#)
- [43] Marius-Constantin Popescu, Valentina E Balas, Liliana Perescu-Popescu, and Nikos Mastorakis. Multilayer perceptron and neural networks. *WSEAS Transactions on Circuits and Systems*, 8(7):579–588, 2009. [4](#)
- [44] David MW Powers. Evaluation: from precision, recall and f-measure to roc, informedness, markedness and correlation. *arXiv preprint arXiv:2010.16061*, 2020. [2](#)
- [45] Can Qin, Shu Zhang, Ning Yu, Yihao Feng, Xinyi Yang, Yingbo Zhou, Huan Wang, Juan Carlos Niebles, Caiming Xiong, Silvio Savarese, et al. Unicontrol: A unified diffusion model for controllable visual generation in the wild. *arXiv preprint arXiv:2305.11147*, 2023. [2](#), [3](#)
- [46] Alec Radford, Jong Wook Kim, Chris Hallacy, Aditya Ramesh, Gabriel Goh, Sandhini Agarwal, Girish Sastry, Amanda Askell, Pamela Mishkin, Jack Clark, et al. Learning transferable visual models from natural language supervision. In *International conference on machine learning*, pages 8748–8763. PMLR, 2021. [3](#), [4](#), [6](#)
- [47] Aditya Ramesh, Mikhail Pavlov, Gabriel Goh, Scott Gray, Chelsea Voss, Alec Radford, Mark Chen, and Ilya Sutskever. Zero-shot text-to-image generation. In *International conference on machine learning*, pages 8821–8831. Pmlr, 2021. [1](#)
- [48] René Ranftl, Katrin Lasinger, David Hafner, Konrad Schindler, and Vladlen Koltun. Towards robust monocular depth estimation: Mixing datasets for zero-shot cross-dataset transfer. *IEEE transactions on pattern analysis and machine intelligence*, 44(3):1623–1637, 2020. [1](#), [2](#)
- [49] Joseph Redmon, Santosh Divvala, Ross Girshick, and Ali Farhadi. You only look once: Unified, real-time object detection. In *Proceedings of the IEEE conference on computer vision and pattern recognition*, pages 779–788, 2016. [1](#), [7](#), [8](#), [9](#)
- [50] Robin Rombach, Andreas Blattmann, Dominik Lorenz, Patrick Esser, and Björn Ommer. High-resolution image synthesis with latent diffusion models. In *Proceedings of the IEEE/CVF conference on computer vision and pattern recognition*, pages 10684–10695, 2023. [1](#), [2](#), [4](#), [5](#), [6](#), [7](#)
- [51] Harrison Rosenberg, Shima Ahmed, Guruprasad Ramesh, Kassem Fawaz, and Ramya Korlakai Vinayak. Limitations of face image generation. In *Proceedings of the AAAI Conference on Artificial Intelligence*, pages 14838–14846, 2024. [9](#)
- [52] Nataniel Ruiz, Yuanzhen Li, Varun Jampani, Yael Pritch, Michael Rubinstein, and Kfir Aberman. Dreambooth: Fine tuning text-to-image diffusion models for subject-driven generation. In *Proceedings of the IEEE/CVF conference on computer vision and pattern recognition*, pages 22500–22510, 2023. [2](#)
- [53] Chitwan Saharia, William Chan, Saurabh Saxena, Lala Li, Jay Whang, Emily L Denton, Kamyar Ghasemipour, Raphael Gontijo Lopes, Burcu Karagol Ayan, Tim Salimans,

- et al. Photorealistic text-to-image diffusion models with deep language understanding. *Advances in neural information processing systems*, 35:36479–36494, 2022. **1**
- [54] Christoph Schuhmann, Romain Beaumont, Richard Vencu, Cade Gordon, Ross Wightman, Mehdi Cherti, Theo Coombes, Aarush Katta, Clayton Mullis, Mitchell Wortsman, et al. Laion-5b: An open large-scale dataset for training next generation image-text models. *Advances in Neural Information Processing Systems*, 35:25278–25294, 2022. **2, 6**
- [55] Maximilian Seitzer. pytorch-fid: FID Score for PyTorch. <https://github.com/mseitzer/pytorch-fid>, 2020. Version 0.3.0. **10**
- [56] Shuai Shao, Zeming Li, Tianyuan Zhang, Chao Peng, Gang Yu, Xiangyu Zhang, Jing Li, and Jian Sun. Objects365: A large-scale, high-quality dataset for object detection. In *Proceedings of the IEEE/CVF international conference on computer vision*, pages 8430–8439, 2019. **2, 6, 7**
- [57] Piyush Sharma, Nan Ding, Sebastian Goodman, and Radu Soricut. Conceptual captions: A cleaned, hypernymed, image alt-text dataset for automatic image captioning. In *Proceedings of the 56th Annual Meeting of the Association for Computational Linguistics (Volume 1: Long Papers)*, pages 2556–2565, 2018. **2, 6, 7**
- [58] Jascha Sohl-Dickstein, Eric Weiss, Niru Maheswaranathan, and Surya Ganguli. Deep unsupervised learning using nonequilibrium thermodynamics. In *International conference on machine learning*, pages 2256–2265. PMLR, 2015. **2, 5**
- [59] Yang Song and Stefano Ermon. Generative modeling by estimating gradients of the data distribution. *Advances in neural information processing systems*, 32, 2019. **2**
- [60] Yang Song, Jascha Sohl-Dickstein, Diederik P Kingma, Abhishek Kumar, Stefano Ermon, and Ben Poole. Score-based generative modeling through stochastic differential equations. *arXiv preprint arXiv:2011.13456*, 2020. **2**
- [61] Wei Sun and Tianfu Wu. Image synthesis from reconfigurable layout and style. In *Proceedings of the IEEE/CVF International Conference on Computer Vision*, pages 10531–10540, 2019. **2, 3**
- [62] Wei Sun and Tianfu Wu. Learning layout and style reconfigurable gans for controllable image synthesis. *IEEE transactions on pattern analysis and machine intelligence*, 44(9): 5070–5087, 2021. **7, 8, 10**
- [63] Tristan Sylvain, Pengchuan Zhang, Yoshua Bengio, R Devon Hjelm, and Shikhar Sharma. Object-centric image generation from layouts. In *Proceedings of the AAAI Conference on Artificial Intelligence*, pages 2647–2655, 2021. **2, 10**
- [64] Igor Vasiljevic, Nick Kolkin, Shanyi Zhang, Ruotian Luo, Haochen Wang, Falcon Z Dai, Andrea F Daniele, Mohammadreza Mostajabi, Steven Basart, Matthew R Walter, et al. Diode: A dense indoor and outdoor depth dataset. *arXiv preprint arXiv:1908.00463*, 2019. **1, 2**
- [65] Ashish Vaswani, Noam Shazeer, Niki Parmar, Jakob Uszkoreit, Llion Jones, Aidan N Gomez, Łukasz Kaiser, and Illia Polosukhin. Attention is all you need. *Advances in neural information processing systems*, 30, 2017. **2**
- [66] Johannes Von Oswald, Christian Henning, Benjamin F Grewe, and João Sacramento. Continual learning with hypernetworks. *arXiv preprint arXiv:1906.00695*, 2019. **3**
- [67] Tengfei Wang, Ting Zhang, Bo Zhang, Hao Ouyang, Dong Chen, Qifeng Chen, and Fang Wen. Pretraining is all you need for image-to-image translation. *arXiv preprint arXiv:2205.12952*, 2022. **2**
- [68] Xudong Wang, Trevor Darrell, Sai Saketh Rambhatla, Rohit Girdhar, and Ishan Misra. Instancediffusion: Instance-level control for image generation. In *Proceedings of the IEEE/CVF Conference on Computer Vision and Pattern Recognition*, pages 6232–6242, 2024. **2, 3**
- [69] Jinheng Xie, Yuexiang Li, Yawen Huang, Haozhe Liu, Wentian Zhang, Yefeng Zheng, and Mike Zheng Shou. Boxdiff: Text-to-image synthesis with training-free box-constrained diffusion. In *Proceedings of the IEEE/CVF International Conference on Computer Vision*, pages 7452–7461, 2023. **3**
- [70] Saining Xie and Zhuowen Tu. Holistically-nested edge detection. In *Proceedings of the IEEE international conference on computer vision*, pages 1395–1403, 2015. **1**
- [71] Zuopeng Yang, Daqing Liu, Chaoyue Wang, Jie Yang, and Dacheng Tao. Modeling image composition for complex scene generation. In *Proceedings of the IEEE/CVF Conference on Computer Vision and Pattern Recognition*, pages 7764–7773, 2022. **2, 3, 7, 8, 10**
- [72] Zhengyuan Yang, Jianfeng Wang, Zhe Gan, Linjie Li, Kevin Lin, Chenfei Wu, Nan Duan, Zicheng Liu, Ce Liu, Michael Zeng, et al. Reco: Region-controlled text-to-image generation. In *Proceedings of the IEEE/CVF Conference on Computer Vision and Pattern Recognition*, pages 14246–14255, 2023. **2, 3**
- [73] Lvmin Zhang, Anyi Rao, and Maneesh Agrawala. Adding conditional control to text-to-image diffusion models. In *Proceedings of the IEEE/CVF International Conference on Computer Vision*, pages 3836–3847, 2023. **2, 3, 4, 5**
- [74] Bo Zhao, Lili Meng, Weidong Yin, and Leonid Sigal. Image generation from layout. In *Proceedings of the IEEE/CVF Conference on Computer Vision and Pattern Recognition*, pages 8584–8593, 2019. **2, 3**
- [75] Shihao Zhao, Dongdong Chen, Yen-Chun Chen, Jianmin Bao, Shaozhe Hao, Lu Yuan, and Kwan-Yee K Wong. Uni-controlnet: All-in-one control to text-to-image diffusion models. *Advances in Neural Information Processing Systems*, 36, 2024. **2, 3, 4**
- [76] Bolei Zhou, Hang Zhao, Xavier Puig, Sanja Fidler, Adela Barriuso, and Antonio Torralba. Scene parsing through ade20k dataset. In *Proceedings of the IEEE conference on computer vision and pattern recognition*, pages 633–641, 2017. **1, 2**